JOURNAL OF MATERIALS SCIENCE **39** (2004) 1987– 1995

Preparation and characterization of new niobophosphate glasses in the Li_2O-Nb_2O_5-CaO-P_2O_5 system

ITALO ODONE MAZALI*
Laboratório de Química do Estado Sólido, Instituto de Química, UNICAMP, P.O.B. 6154, 13084-971 Campinas, SP, Brazil

LUIZ CARLOS BARBOSA
Instituto de Física Gleb Wataghin, UNICAMP, P.O.B. 6165, 13083-970 Campinas, SP, Brazil

OSWALDO LUIZ ALVES‡
Laboratório de Química do Estado Sólido, Instituto de Química, UNICAMP, P.O.B. 6154, 13084-971 Campinas, SP, Brazil
E-mail: oalves@iqm.unicamp.br; http://lqes.iqm.unicamp.br

In the present work we describe the synthesis, spectroscopy, thermal and chemical durability properties of the vitreous system Li_2O-Nb_2O_5-CaO-P_2O_5 (LNCP). Investigations of the short-range order by Fourier transform infrared, Raman, UV-VIS and ^{31}P MAS-NMR spectroscopies suggest that the network former glass consists of Nb octahedra linked to pyro/orthophosphate units through Nb–O–P bonds. The presence of modifier cations (Li^+ and Ca^{2+}) promotes depolymerization of the P–O–P chains, yielding pyro/orthophosphate units. The presence of this kind of structure accounts for the improvement of the chemical durability at low pH when the Nb content in the LNCP glass composition is high. The density and linear refractive indices of LNCP glasses increased linearly as the Nb_2O_5/P_2O_5 molar ratio increased, as a consequence of P_2O_5 substitution by Nb_2O_5 as the glassformer. The dependence of the glass transition temperature, the softening temperature and the crystallization temperature on the Nb_2O_5/P_2O_5 ratio exhibits the same behavior. On the other hand, the thermal expansion coefficient decreases with the increased Nb_2O_5/P_2O_5 ratio.

1. Introduction

Phosphate glasses have received considerable attention in the past few years due to the synthesis of new glass compositions with high chemical stability. The improvement of chemical stability [1–3] stimulated the application of phosphate glasses in several fields of materials science, such as fast ionic conductors [4], semiconductors [5], photonic materials [6–9], hermetic seals [10], rare-earth ion host solid state lasers [11] and biomedical materials [12]. Calcium niobophosphate glasses can be used as precursors to porous glass-ceramics with potential applications in the preparation of integrated chemical systems and nanocomposites [13]. Recently, we reported the fabrication of high performance waveguides by ion exchange (Ag^+/Na^+) in a Na_2O-P_2O_5-PbO-Nb_2O_5 glass substrate [14], which is chemically more durable than commercially available glasses [3].

The properties of the phosphate glasses are determined by the bond polarizability, which depends on their microscopic structures [7] and the network former. For example, the Na_2O-TiO_2-P_2O_5 system presents a high non-linear refractive index that is explained in terms of modification of the glass-forming network determined by the polarizability of the cation and anion bonds and by the presence of Ti in tetrahedral and/or octahedral sites [6–8]. Raman spectra of niobium silicate glass indicate that even a small addition of Nb_2O_5 causes a strong polarized band to appear in the region of 800–900 cm^{-1} [8]. This band has been ascribed to Nb^{5+} in an octahedra site. Lines has studied the influence of the empty d-orbital on the linear and nonlinear refractive indices of transparent transition-metal oxides, based on a bond-orbital theory, and that these results reveal that the most influential ions for the objective of increasing refractive indices are Ti^{4+}, Nb^{5+} and W^{6+} and these are viable additives in this context [15, 16]. Niobophosphate glass compositions such as P_2O_5-Nb_2O_5-V_2O_5-TiO_2 and P_2O_5-Nb_2O_5-V_2O_5-Fe_2O_3, investigated by vibrational spectroscopy,

*Dedicated to the memory of Italo Mazali.
‡Author to whom all correspondence should be addressed.

TABLE I Nominal composition of Li_2O-Nb_2O_5-CaO-P_2O_5 glasses

Mol%				
Li_2O	Nb_2O_5	CaO	P_2O_5	Nomenclature
4	8	43	45	LNCP1
6	18	43	33	LNCP2
4	12	51	33	LNCP3
4	16	51	29	LNCP4
0	16	51	33	NCP5

exhibit structural features, characterized by NbO_4 and NbO_6 units [17]. Since several niobophosphate glasses are Nb-rich and Li-rich, their application as precursors to glass composites containing embedded $LiNbO_3$ ferroelectric crystals has been proposed [18].

In this work, we present a study of the properties of Li_2O-Nb_2O_5-CaO-P_2O_5 glass systems as a function of the Nb_2O_5/P_2O_5 molar ratio, with emphasis on their thermal behavior, structural features, optical and chemical durability properties.

2. Experimental

2.1. Glass preparation

The compositions of Li_2O-Nb_2O_5-CaO-P_2O_5 (LNCP) glasses prepared in this study are summarized in Table I. The raw materials used were reagent-grade Li_2CO_3 (Riedel), $CaCO_3$ (Merck), P_2O_5 (Riedel) and Nb_2O_5 (supplied by the Companhia Brasileira de Metalurgia e Mineração–CBMM). Batches of 25 g were melted at 1350°C for 1 h under air, in platinum crucibles placed in an electric furnace. The mixture was stirred during the melting process in order to obtain homogeneous concentrations. The melts were poured onto carbon plates and annealed at 550°C for 1 h.

2.2. Physical measurements

Powder X-ray diffraction (XRD) patterns were obtained using a Shimadzu XD3A difractometer, with Ni filters and Cu K_α radiation, using 30 kV and 20 mA, calibrated with Si at a 2°/min rate. The density of each glass was measured by the Archimedes's method using deionized water as the buoyancy liquid at 25°C.

The thermal properties were measured by differential thermal analysis (DTA) (Shimadzu model 50WS) under an argon atmosphere (20 mL min^{-1}) and by thermal mechanical analysis (TMA) (Shimadzu model 50WS), which yielded the coefficient of thermal expansion (κ) and the softening temperature (T_d), both at a 10°C min^{-1} heating rate. LNCP2 powdered samples, for testing in the Netzsch 402E dilatometer, were prepared with 5 mm thickness. The heating rate was 10°C min^{-1} and the atmosphere was dry synthetic air, flowing at 30 mL min^{-1}.

Infrared spectra (IR) of KBr pellets were measured with a Perkin Elmer 1600 FTIR in the 1500–400 cm^{-1} range, with a resolution of 4 cm^{-1}. The Raman spectra were recorded on a Renishaw System 3000 Raman Imaging Microscope (ca. 1 μm spatial resolution) using a He-Ne laser (632.8 nm) and 8 mW of power before the entrance optics. ^{31}P MAS-NMR powder spectra were acquired using a Bruker AC-300/P spectrometer operating at 121 MHz and a magnetic field of 7.05 T. Spectra were recorded using acquisition and relaxation times of 0.1 and 2.0 s, respectively. Chemical shifts are referenced to H_3PO_4 (85% in water). In general, chemical shifts were independent of the experimental parameters.

Absorption spectra (200–1500 nm) were obtained on a Hitachi U2000. The linear refractive indexes (η) were measured using a prism-coupling method at 632.8, 1305.4 and 1536.0 nm on polished glass samples. A Metricon model 2010 Prism Coupler instrument, with index accuracy of 0.001, was used.

2.3. Chemical durability evaluation

The chemical durability of the bulk niobophosphate glasses was evaluated from the weight loss versus time of polished glass slabs immersed in 100 mL of 1.0 mol L^{-1} aqueous HCl solution at 25°C in polypropylene beakers [9, 19, 20]. Each measurement, at the different corrosion times, was made on a single sample. After each dissolution period, the slabs were removed from the beaker using polypropylene tweezers, dried on an absorbed paper and weighed. Since the weight loss was linear with time for each glass composition, the chemical durability is expressed as the slope of the curve, in g cm^{-2} min^{-1}. The surface area of polished glass slabs was measured using a micrometer. A modified phosphomolybdate method proposed by Bernhart and Wreath [21] and atomic absorption techniques determined phosphorus and calcium concentrations, respectively, in the leaching solutions.

3. Results and discussion

3.1. Glass formation and density measurements

The preparation procedure described in the experimental section permitted us to obtain bubble-free transparent glasses with high homogeneity and a yellowish color. All the compositions showed XRD patterns typical for a glass phase, presenting a halo near $2\theta = 24.5°$.

Fig. 1 shows the dependence of the density as a function of the $f_{Nb_2O_5}/f_{P_2O_5}$ ratio, where $f_{M_2O_5}$ is the molar

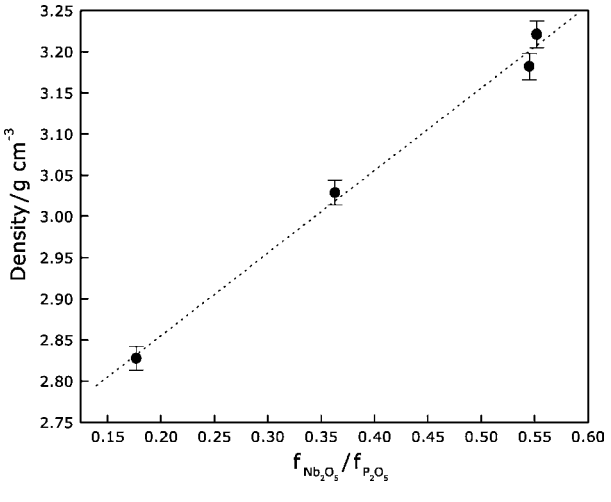

Figure 1 Variation of the density of the LNCP glass systems as a function of the $f_{Nb_2O_5}/f_{P_2O_5}$ ratio.

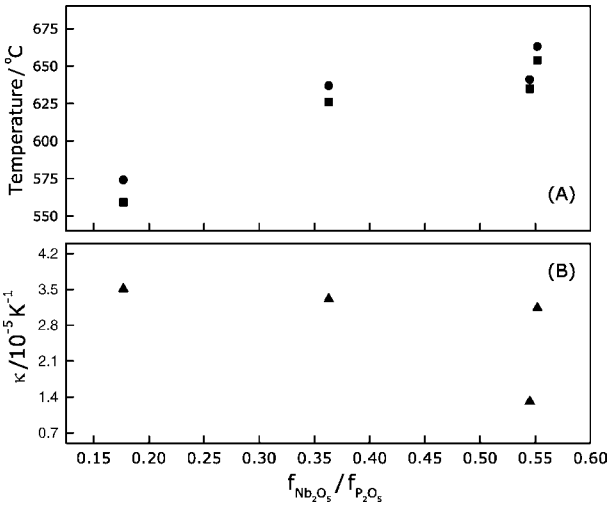

Figure 2 Thermal properties of the LNCP glass system as a function of the $f_{Nb_2O_5}/f_{P_2O_5}$ ratio. The transition (T_g; ■) and softening (T_d; ●) glass temperatures are shown in (A) and the thermal expansion coefficient (κ; ▲) in (B).

fraction of M_2O_5 (M = P, Nb) oxide in the glass composition.

The density values increase linearly as the $f_{Nb_2O_5}/f_{P_2O_5}$ ratio increases. The linear behavior may be explained by substitution of P_2O_5 by the heavier Nb_2O_5. The value of the oxygen molar volume, $V_0 = 12.6 \pm 0.1$ cm^3, calculated according to [22], is independent of the glass composition. This is an indication that Nb_2O_5 acts as a network former in the compositions studied.

3.2. Thermal behavior

The glass transition temperature (T_g), the softening temperature (T_d) and the thermal expansion coefficient (κ) are shown in Fig. 2, as a function of the $f_{Nb_2O_5}/f_{P_2O_5}$ ratio. The influence of the $f_{Nb_2O_5}/f_{P_2O_5}$ ratio of the dilatometric properties of the LNCP glass system are best seen if the comparison is made between the LNCP1 and LNCP2 samples and the LNCP3 and LNCP4 samples because, in both pairs, the CaO and Li_2O contents were kept constant.

The T_g and T_d temperatures increase with the increase in the $f_{Nb_2O_5}/f_{P_2O_5}$ ratio, whereas κ shows a decrease with the $f_{Nb_2O_5}/f_{P_2O_5}$ ratio. An increase in T_g and T_d usually indicates a more closed glass network, whereas a decrease in κ indicates stronger bonds, as stronger bonds decrease the anharmonic contributions of the inter-ionic potentials to thermal expansion. The entrance of Nb_2O_5 in the glass structure as a glass-former may explain the observed dependence on the $f_{Nb_2O_5}/f_{P_2O_5}$ ratio. The difference between T_g and T_d, for the whole composition range, is roughly constant, as shown by Fig. 2.

DTA curves for all LNCP compositions are shown in Fig. 3 and it is evident that the devitrification behavior depends on the glass composition. Typical glass parameters: T_x (the onset of crystallization temperature) and T_c (crystallization temperature) were extracted from these curves (Fig. 3) and are summarized in Table II.

That LNCP1 glass exhibits a broad and weak crystallization peak points out the presence of a polymeric structure as a consequence of the high P_2O_5 content. LNCP1 and LNCP3 glasses show two crystallization peaks in the region of 770–830°C, however, samples containing higher niobium amounts (LNCP2 and LNCP4) present a single crystallization peak at 830°C. This observation suggests a shift of the first crystallization peak to higher temperatures as a consequence of the increasing niobium content. It is important to note the presence of a distinct shoulder at 815°C for LNCP2 glass (Fig. 3), indicating the occurrence of an additional thermal event. The increase of stretching bond of network glass with the increase in the $f_{Nb_2O_5}/f_{P_2O_5}$ ratio may explain the higher T_c observed for the LNCP glass system.

It is noteworthy that when lithium ions are absent from the glass composition, the crystallization temperatures are higher by almost 80°C than in the presence of Li_2O (NCP5 compared with LNCP4 glass, because the Nb_2O_5 and CaO contents were kept constant). DTA measurements of glass samples indicate that lithium ions play an important role in the devitrification of the LNCP system, decreasing the initial temperature of crystallization. Replacing a P_2O_5 network former by monovalent ions increases the depolymerization of the glass network and facilitates nucleation and crystallization because the Li^+ ion cannot ionically bridge two non-bridging oxygens [23].

The pronounced endothermic effect in the DTA curve (Fig. 4a), which appeared just before the devitrification event, can be explained as a result of softening and sintering of the powdered LNCP glass. As a matter of fact, the initially powdered sample was recovered from the sample holder as dense monolith. The DTA curve

TABLE II Values of the $f_{Nb_2O_5}/f_{P_2O_5}$ ratio, T_x and T_c for the glasses of the Li_2O-Nb_2O_5-CaO-P_2O_5 system, with different compositions

Glass	$f_{Nb_2O_5}/f_{P_2O_5}$	T_x^1	T_c^1	T_x^2	T_c^2
LNCP1	0.177	737	771	802	818
LNCP2	0.545	–	–	791	830
LNCP3	0.363	760	775	811	825
LNCP4	0.552	–	–	804	830
NCP5	0.484	835	857	895	895

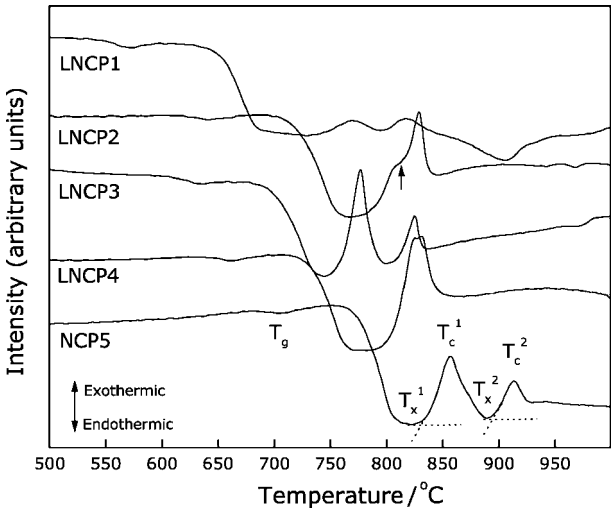

Figure 3 DTA curves of the LNCP glass systems.

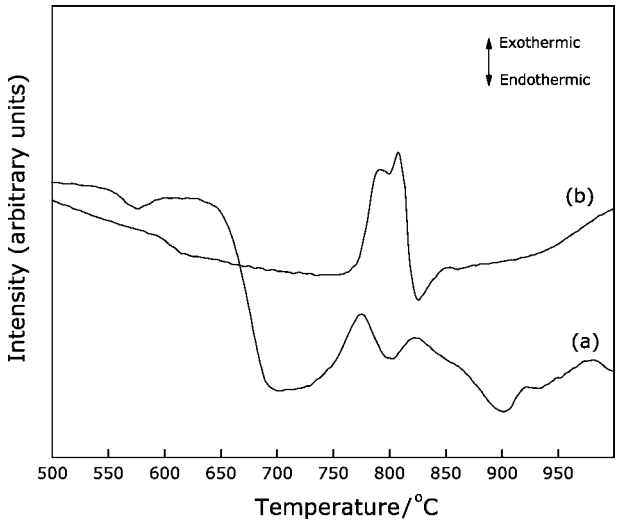

Figure 4 DTA curves for the LNCP1 glass, with samples in the: (a) powder and (b) monolithic forms.

of Fig. 4b was measured for a monolithic glass sample (the powdered glass was melted at 1350°C in sample holder of DTA for 1 h and annealed at 550°C for 1 h, to obtain monolithic glass *in situ* in sample holder) and the softening phenomena are not observed. Mazali and Alves [13] demonstrated that the devitrification of monolithic LNCP glass occurs by surface crystallization, through heterogeneous nucleation, and the process proceeds from the surface to the bulk of the specimen. In this particular case, the increase of surface area of LNCP glass does not represent any change in nucleation mechanism. Fresa and coworkers [24] showed that the $(2.5-x)$CaO-$(x/3)Y_2O_3$-$2SiO_2$ glass system exhibit a slope change in DTA curve just before the devitrification process, as a result of softening and sintering.

Fig. 5 shows the linear shrinkage $(\Delta L/L_0)$ and the linear shrinkage rate $[\mathrm{d}(\Delta L/L_0)/\mathrm{d}T]$ as a function of temperature for LNCP2 glass, which exhibits the maximum shrinkage rate at 745°C. In glass, sintering take place by the viscous flow of a glass phase [25] and the densification phenomena occur by coalescence process, which starts with the formation of necks between particles. The desired characteristic of glass is achieved by sintering to full densification. The negative variation of

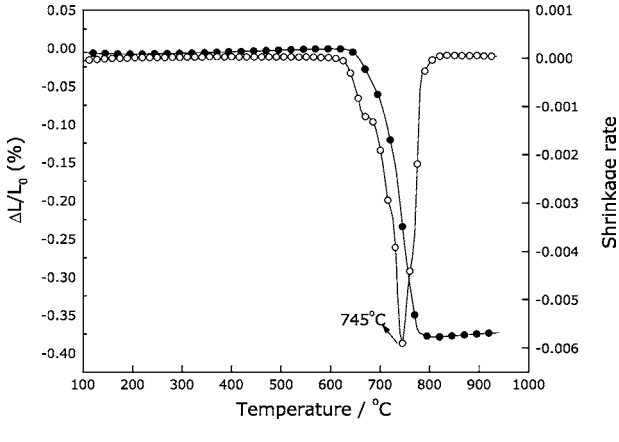

Figure 5 (●) Linear shrinkage $(\Delta L/L_0)$ and (○) linear shrinkage rate as a function of temperature for LNCP2 glass.

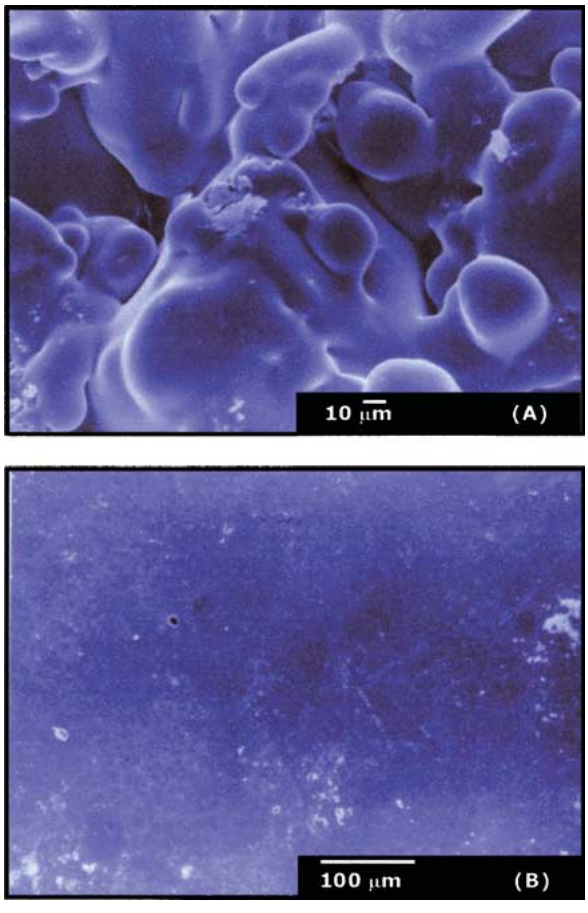

Figure 6 SEM micrograph of the fracture face of compacted powdered LNCP2 glass after thermal treatment at 745°C for: (A) 2 min and (B) 15 min.

the linear shrinkage $(\Delta L/L_0)$ indicates the occurrence of densification. Scanning electron microscopy (SEM) (Fig. 6a) of compacted powdered LNCP2 glass after thermal treatment at 745°C for 2 min shows the softening of the glass and the coalescence between particles; after 15 min at 745°C, no crystallization is observed (by XRD) but there is some residual porosity (Fig. 6b). This result confirmed the occurrence of the sintering process followed by densification in powdered calcium niobophosphate glasses.

This result clearly indicates that it is possible to obtain monolithic shaped into a particular form from isostatically pressed powder glass samples, using thermal treatments in the range of 700–750°C. Porous monolithic ceramics or glasses have been widely used in several fields such as filters, catalysis supports and biochemical applications [26–30]. The porous monolith also performs the important role as support in integrated chemical system [31, 32]. The fabrication of porous monolith by powder glass sintering permits the control of pore features by changing parameters, such as: particle size, time and temperature of sintering, and addition of foaming agents ($NaHCO_3$, $CaCO_3$, $NH_4H_2PO_4$, cellulose) with different concentrations [33, 34].

3.3. IR and Raman spectra

The predominant phosphate groups present in LNCP1 and LNCP2 glasses were investigated by IR and Raman

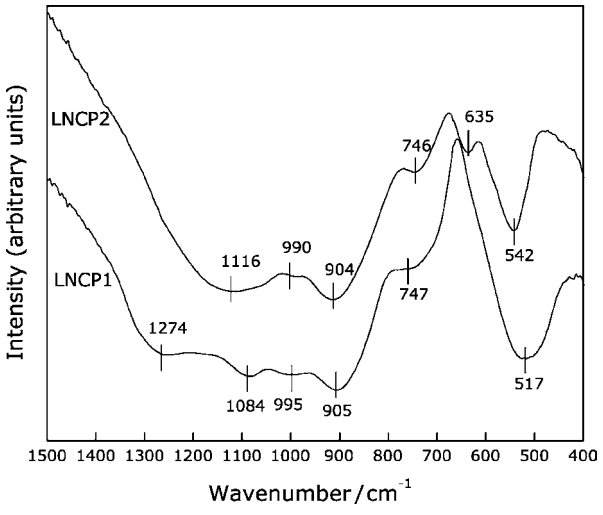

Figure 7 IR spectra of LNCP1 and LNCP2 glasses.

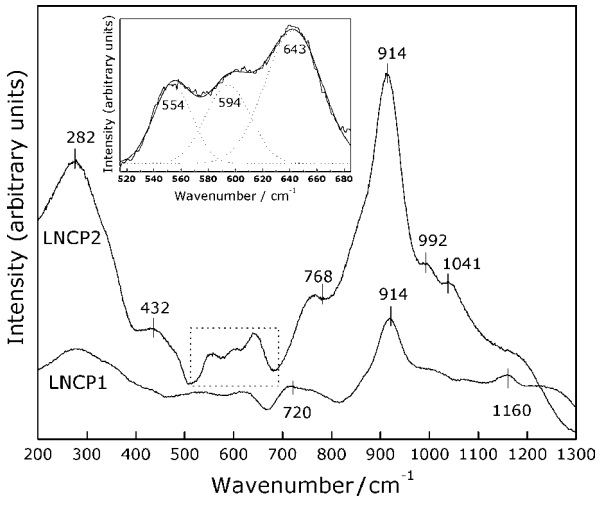

Figure 8 Raman spectra of LNCP1 and LNCP2 glasses.

spectroscopies (Figs 7 and 8). The IR and Raman spectra of LNCP2 glass are representative of the other glass samples. The IR and Raman bands and tentative assignments are summarized in Table III. Bands at 1274 and 1084 cm^{-1} in the IR spectrum of LNCP1 can be assigned, respectively, to antisymmetric and symmetric PO_2 stretching [35]. Bands at 1274 and 995 cm^{-1} can be assigned, respectively, to PO^- and PO_4^{3-}, showing depolymerization of polyphosphate chains as a result of the presence of the alkaline ions (Li^+ and Ca^{2+}) for both samples [35]. Bands at 905 and 747 cm^{-1} are assigned to antisymmetric and symmetric stretching of P—O—P units, indicating that chain structures are still present, regardless of the occurrence of depolymerization.

TABLE III The position and tentative assignment of IR and Raman bands for the LNCP1 and LNCP2 glasses

Band location (cm^{-1})				
IR		Raman		
LNCP1	LNCP2	LNCP1	LNCP2	Tentative assignment
1274(s)				$\upsilon_{as}(PO_2)$ and/or υ(P═O)
	1116(s)		1041(sh)	$\upsilon_s(PO_3^{2-})$
1084(s)		1160(w)		$\upsilon_s(PO_2)$
995(s)	990(s)			$\upsilon(PO_4^{3-})$
747(sh)	746(sh)	720(w)		υ_s(POP)
			992(sh)	υ_{as}(POP)
905(s)	904(s)	914(m)	914(vs)	γ_{Nb-O} (short Nb—O distances)
	635(w)		768(sh)	γ_{Nb-O} (medium Nb—O
	542(m)		643(w)	distances) + $\delta_{(O-P-O)}$
			594(w)	
			554(w)	
517(s)		282(m)	282(s)	$\delta_{(O-P-O)} + \delta_{(O-Nb-O)}$

vs = very strong, s = strong, m = medium, w = weak, and sh = shoulder.

According to Tatsumisago and coworkers [36] the presence of terminal PO_2^- and PO_3^{2-} groups is characteristic of open-chain metaphosphates since, for cyclic metaphosphates, bands assigned to terminal PO_3^{2-} are not observed. Bands assigned to the PO_2^- group are absent for ortho and pyrophosphates.

The predominant structure of LNCP1 glass contains metaphosphate chains, as shown by the absence of orthophosphate bands and by the presence of PO_3^{2-} and PO_2^- bands [37]. The LNCP2 glass composition presents a rather different IR spectrum. Apart from the presence of P—O—P and PO_3^{2-} bands, indicative of condensed phosphates, bands associated with orthophosphate units are present. In addition, the absence of PO_2^- bands indicates that this glass composition presents ortho and pyrophosphate units as the major components, in agreement with the higher concentration of alkaline ions than in LNCP1 glass.

For all compositions, an IR band observed at ca. 905 cm^{-1} can be assigned to the short distance Nb—O symmetrical stretching of NbO_6 octahedra [38, 39].

The above statements are confirmed by the Raman spectra, shown in Fig. 8. For the LNCP1 glass, bands at 720 and 1160 cm^{-1} are assigned, respectively, to P—O—P and PO_2 symmetric stretching from metaphosphate chains. According to Jazouli and coworkers [38, 39], the introduction of niobium in the glass network results in an intense Raman band near 900 cm^{-1}, observed at 914 cm^{-1} for LNCP1 and LNCP2, assigned to short Nb—O bonds from NbO_6 octahedra. The intensity of the band at 914 cm^{-1} increases with the increasing $f_{Nb_2O_5}/f_{P_2O_5}$ ratio, in contrast to the decrease of intensity observed for the bands at 720 and 1160 cm^{-1}. For the LNCP2 glass, which has a $f_{Nb_2O_5}/f_{P_2O_5}$ ratio equal 0.545, the bands at 720 and 1160 cm^{-1} are no longer observed, indicating the substitution of PO_2^- intrachain groups by octahedra units containing Nb.

Concerning Nb—O vibrations, Raman and IR spectra of LNCP1 and LNCP2 glasses present pronounced differences. As already mentioned, bands at 905 cm^{-1} (IR) and 914 cm^{-1} (Raman) are assigned to symmetrical stretching of short distance Nb—O bonds from NbO_6 octahedra. The IR band observed for LNCP1 at 517 cm^{-1} and the Raman bands at 282 and 532 cm^{-1} are assigned to [(O—P—O) + (O—Nb—O)] coupled deformation modes. For LNCP2, IR bands at 635 and 542 cm^{-1} and Raman bands at 554, 594, 643 and 768 cm^{-1} are assigned to the vibrational coupling of [(Nb—O) (medium Nb—O distances) + (O—P—O)] stretching with deformation modes [38, 39]. The Raman band at 282 cm^{-1} is also observed for LNCP2. These observations suggest the role of Nb^{5+} ions as the glassformer in LNCP glasses. In glass

compositions containing small amounts of Nb (LNCP1; $f_{Nb_2O_5}/f_{P_2O_5} = 0.177$), the presence of low intensity bands associated with short Nb–O bonds reveals a dispersive distribution of this element in the network, which acts as an ionic cross-link between metaphosphate chains. On the other hand, for niobium-rich compositions with the $f_{Nb_2O_5}/f_{P_2O_5}$ ratio changing from 0.363 to 0.552, the niobium amount inside the glass chains increases because the non-bridging oxygens of NbO_6 octahedra act as ionic cross-links between ortho and pyrophosphate chains. According to Vogel and coworkers [40], in silicate glasses, Nb^{5+} in an octahedra site creates five non-bridging oxygens per cation. Therefore, the niobophosphate glasses studied here are predominantly (except LNCP1 glass) made up of short chain phosphate anions (pyrophosphate) linked through Nb–O–P bonds. For such a structure, it is evident that divalent cations can serve as ionic cross-links between the non-bridging oxygens (proceeding from NbO_6 octahedra and/or phosphate chains) of two different chains, forming the three-dimensional network.

It is worthy to mention that, in addition to the increase in the $f_{Nb_2O_5}/f_{P_2O_5}$ ratio from LNCP1 to LNCP2, the concentration of the modifier cations (Li^+ and Ca^{2+}) increased, in comparison to the P_2O_5 content. Similar to results reported by Pemberton and coworkers [41], the intensities of the Raman bands at 720, 1160 and 1041 cm^{-1} were sensitive to the increase of modifier cations such as Ca^{2+}, indicating that changing the concentration of every component may affect band shapes.

3.4. ^{31}P MAS-NMR spectra

The Q^n model is a useful approach for analysis of ^{31}P MAS-NMR spectra of phosphate. In pure P_2O_5, the PO_4 tetrahedra are connected at three of the four corners to form a random network structure. As metal cations are added to the structure, non-bridging oxygen bonds are created to preserve charge balance, breaking up the network of PO_4 tetrahedra. A convenient parameter for characterizing the overall structure of these phosphate glasses is Q^n, where n is defined as the average number of non-bridging oxygens per PO_4 tetrahedron. Therefore, the number of bridging oxygens per PO_4 tetrahedron is simply $4 - n$ ($0 \leq n \leq 3$).

Broad isotropic signals, centered at −10.0 ppm (LNCP2), −8.3 ppm (LNCP3) and −2.7 ppm (LNCP4) are shown in Fig. 9. The values of the chemical shifts are consistent with the presence of high amounts of modifiers while the width reveals the typical structural disorder of vitreous systems. The last effect has been explained by an angular dependence different from $(3\cos^2\theta - 1)$ for the local magnetic field, arising from neighboring nucleus amorphous samples, in contrast to crystalline samples for which magic angle spinning removes the dipolar broadening of bands.

The ^{31}P MAS-NMR spectra reveal the predominance of Q^1 units belonging to pyrophosphate chains, in agreement with IR and Raman data. According to the ^{31}P MAS-NMR spectra, the exception is the composition LNCP1, which exhibits a spectrum typical of a metaphosphate structure [42].

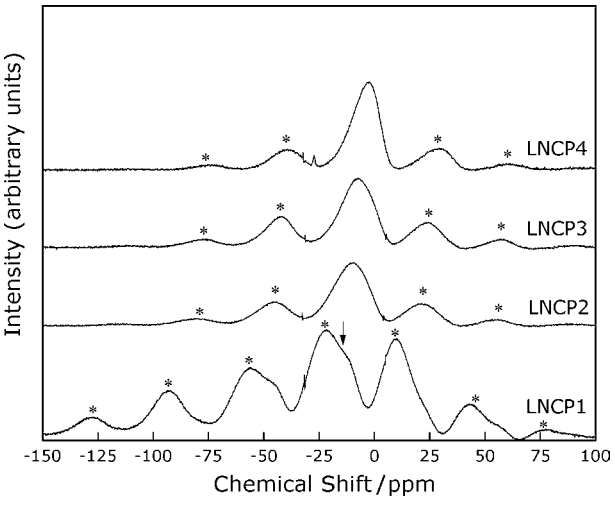

Figure 9 ^{31}P MAS NMR spectra of LNCP glass systems. Isotropic peaks and spinning side bands in the NMR spectra are denoted by (↓) and (∗), respectively.

Increasing the CaO content in $x\text{CaO}\cdot(90-x)P_2O_5\cdot y\text{TiO}_2\cdot(10-y)\text{Na}_2\text{O}$ glass, the degree of depolymerization of the phosphate chain increases, as expected from the role of the alkaline ions. For a glass composition containing $x = 60$ mol%, with y changing from 0 to 10 mol%, the ^{31}P NMR-MAS spectra shows the existence of only Q^0 (orthophosphate) and Q^1 (pyrophosphate) units in the glass. The intensity of the peak assigned to Q^1 units increases as the TiO_2 content increases, due to the formation of the P–O–Ti linkage [42]. Apart from evidence for the presence of Q^1 units, the existence of Q^0 units cannot be ruled out from the high amount of modifiers. Recently, Montagne and coworkers [43] pointed out that some phosphate glasses containing predominantly Q^1 units can also exhibit Q^0 and Q^2 (metaphosphate), resulting from the equilibrium $2Q^1 \leftrightarrow Q^0 + Q^2$. In this case the amount of Q^0 and Q^2 is strictly equivalent, yielding typical ^{31}P MAS-NMR Q^1 units. As a good approach, these statements can be extended to the niobium-phosphate glasses studied here.

The value of Q^n can be computed directly from the composition of the phosphate glasses and is given by empirical equation [44]

$$n = 3 - \frac{\sum(q \cdot f_M)}{f_P} \quad (1)$$

where f_M is the molar concentration of each element in the glass and f_P is the molar concentration of P. The q value considers the number of non-bridging oxygens that a modifier cation can produce or balance in PO_4 tetrahedra.

It can be considered that NbO_6 octahedra can neutralize only one non-bridging bond in a PO_4 tetrahedra. IR and Raman results and the Zachariasen model support this statement. The first showed that the Nb is localized in a NbO_6 octahedra units in the glass network. The second establishes that the polyhedra responsible for glass network formation must be linked through the corners, only occasionally through the faces or edges. Therefore, from Equation 1, just one NbO_6 octahedra is used

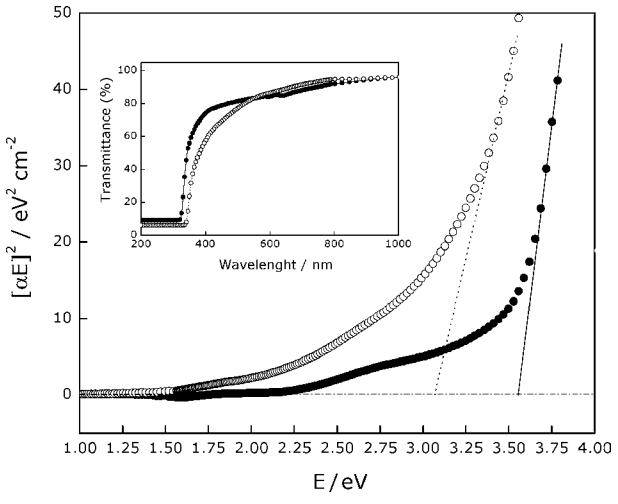

Figure 10 Plot of $(\alpha E)^2$ as a function of photon energy for the (●) LNCP1 and (○) LNCP2 glasses. The solid and dashed lines are the linear fits to obtain the optical gap for the LNCP1 and LNCP2 glass samples, respectively. The inset shows the transmission curves.

to calculate n with charge 1. Applying Equation 1, the LNCP1 and LNCP2 glass samples show $Q^{2(1.8)}$ and $Q^{1(0.97)}$-like structure, respectively. This result shows total agreement with experimental results, hence, confirming the role of Nb as glassformer in the LNCP glass systems.

3.5. Absorption spectra

We have measured glass transmission in the wavelength range 200−1500 nm. The transmittance data are shown in the inset of Fig. 10 for LNCP1 and LNCP2 glass samples. The curves show that these glasses have a high transmittance in the 800−1500 nm region. The curves for the other samples (LNCP3, LNCP4 and NCP5) are indistinguishable from the LNCP2 curve. We assign the cut-off value as the wavelength where the extrapolation of the decay in the transmission curve in the UV region reaches zero transmission. The UV-Vis cut-off wavelength is at 319 and 337 nm for the LNCP1 and LNCP2 glass samples, respectively. The strong absorption thresholds observed correspond to an electronic transfer, which can be schematized [38]:

$$O^{2-}(2p^6) + Nb^{5+}(4d^0) \rightarrow O^{-}(2p^5) + Nb^{4+}(4d^1 t_{2g}) \quad (2)$$

These thresholds are all located at high energies and depend on the $f_{Nb_2O_5}/f_{P_2O_5}$ ratio. From the transmission curve we calculated the optical absorption coefficient, α. In order to obtain the optical energy gap we plotted $(\alpha E)^2$ as a function of E, where E is the photon energy in eV. Fig. 10 shows the curves for the LNCP1 and LNCP2 glass samples. The values of the optical energy gap were obtained from extrapolation of the linear regions of the plots to $(\alpha E)^2 = 0$. The optical gap is ca. 3.55 eV for LNCP1 and ca. 3.07 eV for LNCP2.

As previously pointed out (in Sections 3.3 and 3.4) niobium is present in the glass as NbO_6 octahedra units. These groups share some of their oxygen atoms with PO_4 groups. El Jazouli and coworkers [38] showed that, for glasses with low niobium content, the Nb–O bonds have relatively strong ionic character due to competition with the high amount of PO_4 tetrahedra, leading to a high E threshold. As a consequence, as the niobium content increases and the relative number of PO_4 groups decreases, E is expected to decrease [38]. This behavior has been found for the niobophosphate glasses studied here, since the absorption threshold value obtained for the LNCP1 sample ($f_{Nb_2O_5}/f_{P_2O_5}$ ratio = 0.177) of 3.55 eV decreases to 3.07 eV as the $f_{Nb_2O_5}/f_{P_2O_5}$ ratio increases to 0.545 (LNCP2 sample), as a result of the higher content of Nb–O bonds in the glass structure. For the niobophosphate glasses the absorption threshold is close to that of α-$NbPO_5$, which is consistent with the presence of corner-sharing NbO_6 groups.

The measured linear refractive indices (η) of the LNCP glass system decrease with increasing wavelengths, centered at 632.8, 1305.4 and 1536.0 nm, as shown in Fig. 11. The η, which we expect to follow the density, also increases with the $f_{Nb_2O_5}/f_{P_2O_5}$ ratio.

The η of the glasses are determined by the bond polarizability and a small addition of Nb_2O_5 in the TiO_2-Na_2O-P_2O_5 system causes a strong polarized band to appear in the region of 800−900 cm^{-1}. This band has been assigned to Nb^{5+} in an octahedral site [45]. In this system, the increase of Nb content causes an increase of the linear refractive index. Therefore, the analysis of the Raman data of the LNCP1 and LNCP2 glasses showed an increasing presence of P–O–Nb bonding in the glass with increasing refractive index. Linear refractive index data for similar niobophosphate glasses show that LNCP glass systems exhibit higher η at 632.8 nm, considering the $f_{Nb_2O_5}/f_{P_2O_5}$ ratio: $26Na_2O$-$20Nb_2O_5$-$54P_2O_5$ ($f_{Nb_2O_5}/f_{P_2O_5}$ ratio = 0.37; η = 1.6536) and $35Na_2O$-$5Al_2O_3$–$25Nb_2O_5$-$35P_2O_5$ ($f_{Nb_2O_5}/f_{P_2O_5}$ ratio = 0.71; η = 1.7060) [9].

3.6. Chemical durability

Phosphate glasses often present poor chemical durability in aqueous solution. It has been possible to prepare

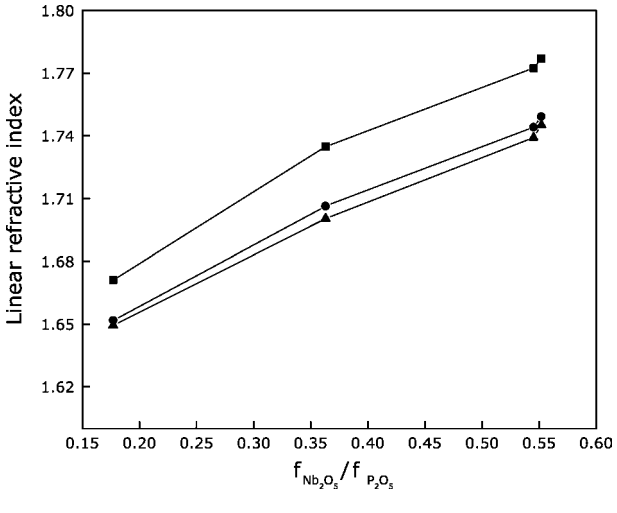

Figure 11 Linear refractive index of the LNCP glass system as a function of the $f_{Nb_2O_5}/f_{P_2O_5}$ ratio. ■ = 632.8 nm; ● = 1305.4 nm and ▲ = 1536.0 nm.

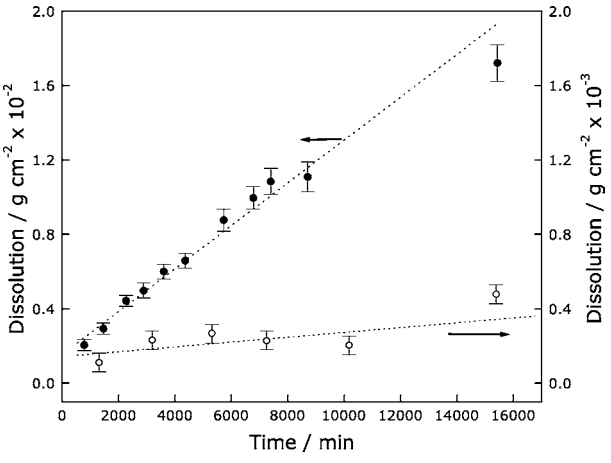

Figure 12 Sample weight losses versus leaching time for the (●) LNCP1 and (○) LNCP2 glasses at 25°C, 1.0 mol L^{-1} HCl aqueous solution. Volume: 100 ml.

phosphate glasses with resistance to aqueous corrosion, comparable to silicate glasses. For example, lead iron phosphate glasses are found to be more durable than borosilicate glasses [46]. The dissolution rate of a phosphate glass is quite sensitive to the glass composition, ranging over more than four orders of magnitude, from over 10^{-4} to almost 10^{-9} g cm^{-2} min^{-1} [19, 20].

Fig. 12 shows the weight losses per unit surface area as a function of time for the LNCP1 and LNCP2 glasses. The glass composition containing a smaller $f_{Nb_2O_5}/f_{P_2O_5}$ ratio (LNCP1) exhibits a very high dissolution rate (1×10^{-6} g cm^{-2} min^{-1}), compared to the niobium-rich composition. The lowest dissolution rate, found for LNCP2 glass, was 5×10^{-8} g cm^{-2} min^{-1}.

Phosphate glasses might dissolve by one of two mechanisms: hydrolysis or hydration reactions. The hydrolysis reaction of covalent P—O—P bonds would eventually result in the destruction of the polymeric phosphate network to produce orthophosphate. On the other hand, a hydration reaction occurs at the modifier cations, disrupting ionic bonds between the phosphate chains [20]. Thus, dissolution mechanism involves hydration of entire chains rather than cleavage of P—O bonds by hydrolysis reactions; the chains dissolve intact [19]. For the LNCP1 sample, an f_P/f_{Ca} ratio of 4 has been found in the leaching solutions, while, for the other samples, a f_P/f_{Ca} ratio near 1.4 was found. This observation provides additional evidence of the presence in LNCP1 glass of phosphate chains longer than in the other glass compositions.

The IR and Raman data suggest that the glass structure consists of Nb octahedra linked to pyrophosphate units through Nb—O—P bonds, which could increase the chemical resistance of niobophosphate glasses by inhibition of the hydrolysis reactions. Therefore, it is possible to improve the chemical durability of the glass by increasing the $f_{Nb_2O_5}/f_{P_2O_5}$ ratio. In addition, the phosphate glasses studied here (except the LNCP1 composition) are predominantly made up of short chain polymeric phosphate anions, which are connected to one another through ionic bonds to the modifier cations. For such a structure, Ca^{2+} ions can serve as an ionic cross-linker between the non-bridging oxygens of two different chains. According to Bunker and coworkers [19], the formation of such cross-links explains why the chemical durability increases as the f_P/f_{Ca} ratio in the glass is reduced, as a consequence of the inhibition of hydration reactions. Therefore, the chemical durability of niobophosphate glasses results from the high degree of depolymerization of chains and because Nb acts as a glassformer in the compositions studied.

4. Conclusion

We have described herein highly homogeneous Li_2O-Nb_2O_5-CaO-P_2O_5 glasses. Investigations of the short-range order by Fourier transform infrared, Raman, UV-VIS and ^{31}P MAS-NMR spectroscopies suggest that the glass structure consists of Nb^{5+} octahedra linked to pyro/orthophosphate units through Nb—O—P bonds, which confer high polarizability to the glass systems. The glass transition, softening and crystallization temperatures, thermal expansion coefficient, density, UV-VIS cut-off, optical gap and linear refractive index were found to depend on the $f_{Nb_2O_5}/f_{P_2O_5}$ ratio. Linear refractive indices data for similar glasses show that the LNCP glass system exhibits higher η at 632.8 nm than reported in the literature. The presence of modifier cations such as Li^+ and Ca^{2+} promote depolymerization of the P—O—P chains, yielding pyro (Q^1) and orthophosphate (Q^0) units. The presence of this kind of structure accounts for the improvement of chemical stability at low pH when the $f_{Nb_2O_5}/f_{P_2O_5}$ ratio in the glass composition increases. We believe that the results are important to establish the chances of practical applications of this glass family in optical devices and as precursors for porous glass-ceramics. Future research will be directed to the study of the nonlinear refractive index and its relation to glass composition.

Acknowledgements

The authors are grateful to FAPESP (Proc. 97/09928-1) for financial support, to the Companhia Brasileira de Metalurgia e Mineração (CBMM) for kindly providing the niobium oxide, to Prof. D. L. A. Faria and Prof. M. L. A. Temperini (Molecular Spectroscopy Laboratory, IQ-USP, São Paulo, Brazil) for Raman measurements and to Dr. Iara de Fátima Gimenez (IQ-UNICAMP, Campinas, Brazil) for English revision. This is a contribution of Millennium Institute for Complex Materials (PADCT/MCT).

References

1. B. C. SALES and L. A. BOATNER, *J. Non-Cryst. Solids* **79** (1986) 83.
2. Y. B. PENG and D. E. DAY, *Glass Technol.* **32** (1991) 166.
3. N. ARANHA, O. L. ALVES, L. C. BARBOSA and C. L. CESAR, in Proc. XVII Int. Congr. Glass, Beijing (1995) Vol. 7, p. 282.
4. G. FUXI, *J. Non-Cryst. Solids* **123** (1990) 385.
5. L. J. BOGOMOLOVA, *ibid.* **30** (1979) 379.
6. S. KRIMI, A. EL JAZOULI, L. RABARDEL, M. COUZI, I. MANSOURI and G. LE FLEM, *J. Solid State. Chem.* **102** (1993) 400.

7. E. M. VOGEL, *J. Amer. Ceram. Soc.* **72** (1989) 719.
8. L. A. FARROW and E. M. VOGEL, *J. Non-Cryst. Solids.* **143** (1992) 59.
9. N. V. NIKONOROV and G. T. PETROVSKII, *Glass Phys. Chem.* **25** (1999) 16.
10. R. K. BROWN and D. R. TALLANT, *J. Non-Cryst. Solids* **222** (1997) 396.
11. D. K. SARDAR, J. B. GRUBER, B. ZANDI, J. A. HUTCHINSON and C. W. TRUSSELL, *J. Appl. Phys.* **93** (2003) 2041.
12. K. FRANKS, V. SALIH, J. C. KNOWLES and I. OLSEN, *J. Mater. Sci.: Mater. Med.* **13** (2002) 549.
13. I. O. MAZALI and O. L. ALVES, *J. Mater. Sci. Lett.* **20** (2001) 2113.
14. L. C. BARBOSA, N. ARANHA, O. L. ALVES and R. SRIVASTAVA, *Electron. Lett.* **32** (1996) 1919.
15. M. E. LINES, *Phys. Rev.* B **41** (1990) 3383.
16. *Idem., ibid.* **43** (1991) 11978.
17. G. E. RACHKOVSKAYA and N. M. BOBKOVA, *J. Non-Cryst. Solids* **90** (1987) 617.
18. E. B. ARAUJO, J. A. C. PAIVA, M. A. B. ARAÚJO and A. S. B. SOMBRA, *Phys. State Solid.* B **197** (1996) 231.
19. B. C. BUNKER, G. W. ARNOLD and J. A. WILDER, *J. Non-Cryst. Solids* **64** (1984) 291.
20. B. S. BAE and M. C. WEINBERG, *Glass Technol.* **35** (1994) 83.
21. D. N. BERNHART and A. R. WREATH, *Anal. Chem.* **27** (1955) 440.
22. L. MONTAGNE, G. PALAVIT and R. DELAVAL, *J. Non-Cryst. Solids* **223** (1998) 43.
23. J. HENRY and R. G. HILL, *ibid.* **319** (2003) 9.
24. R. FRESA, A. COSTANTINI and F. BRANDA, *Thermochim. Acta* **302** (1997) 87.
25. A. A. EL-KHESHEN and M. F. ZAWRAH, *Ceram. Int.* **29** (2003) 251.
26. M. D. M. INNOCENTINI, W. L. ANTUNES, J. B. BAUMGARTNER, J. P. K. SEVILLE and J. R. COURY, *Adv. Powder Technol.* **299**(3) (1999) 19.
27. R. SONDHI and R. BHAVE, *J. Membr. Sci.* **186** (2001) 41.
28. S. NAKAGAKI, A. R. RAMOS, F. L. BENEDITO, P. G. PERALTA-ZAMORA and A. J. G. ZARBIN, *J. Mol. Catal. A: Chem.* **185** (2002) 203.
29. H. M. HULTMAN, M. DE LANG, I. W. C. E. ARENDS, U. HANEFELD, R. A. SHELDON and T. MASCHMEYER, *J. Catal.* **217** (2003) 275.
30. B. J. MELDE and A. STEIN, *Chem. Mater.* **14** (2002) 3326.
31. A. J. BARD, "Integrated Chemical Systems—a Chemical Approach to Nanotechnology" (John Wiley & Sons, New York, 1994) p. 324.
32. I. F. GIMENEZ and O. L. ALVES, *J. Braz. Chem. Soc.* **10** (1999) 167.
33. S. FURUTA, H. NAKAO and H. KATSUKI, *J. Mater. Sci. Lett.* **12** (1993) 286.
34. P. DUCHEYNE, A. EL-GHANNAM and I. SHAPIRO, Patent USA 5.676.720 (1997).
35. C. DAYANAND, G. BHIKSAMAIAH, V. J. TYAGARAJU, M. SALAGRAM and A. S. R. K. MURTHY, *J. Mater. Sci.* **31** (1996) 1945.
36. M. TATSUMISAGO, A. HAMADA, T. MINAMI and M. TANAKA, *J. Non-Cryst. Solids* **56** (1983) 423.
37. A. RULMONT, R. CAHAY, M. LIEGEOIS-DUYCKAERTS and P. TARTE, *Eur. J. Solid State Inorg. Chem.* **28** (1991) 207.
38. A. EL JAZOULI, J. C. VIALA, C. PARENT, G. LE FLEM and P. HAGENMULLER, *J. Solid State Chem.* **73** (1988) 433.
39. A. EL JAZOULI, C. PARENT, J. M. DANCE, G. LE FLEM, P. HAGENMULLER and J. C. VIALA, *ibid.* **74** (1988) 377.
40. E. M. VOGEL, S. G. KOSINSKI, D. M. KROL, J. L. JACKET, S. R. FRIBERG and M. OLIVER, *J. Non-Cryst. Solids* **107** (1989) 244.
41. E. PEMBERTON, L. LATIFZADEH, J. P. FLETCHER and S. H. RISBUD, *Chem. Mater.* **3** (1991) 195.
42. T. KASUGA and Y. ABE, *J. Non-Cryst. Solids* **243** (1999) 70.
43. L. MONTAGNE, G. PALAVIT and G. MAIRESSE, *Phys. Chem. Glasses* **37** (1996) 206.
44. B. C. SALES, *J. Non-Cryst. Solids* **119** (1990) 136.
45. K. FUKUMI and S. SAKKA, *J. Mater. Sci.* **23** (1988) 2819.
46. B. C. SALES and L. A. BOATNER, *J. Non-Cryst. Solids* **79** (1986) 83.

Received 22 May
and accepted 13 November 2003